TERNARY MASS TRANSFER IN A WETTED-WALL COLUMN SIGNIFICANCE OF DIFFUSIONAL INTERACTIONS PART I. STEFAN DIFFUSION

By R. KRISHNA (MEMBER)

Department of Chemical Engineering, University of Manchester Institute of Science and Technology, Manchester, England

This paper examines methods for predicting ternary mass transfer from information on the transport properties of the constituent binary pairs, with a view to determining the significance of diffusional interactions in multicomponent mass transfer. Experimental data obtained by Modine in a wetted-wall column for mass transfer, between a falling film of a binary liquid mixture containing acetone and benzene and a downward flowing ternary vapour–gas mixture containing acetone, benzene and nitrogen or helium, are used to test the validity of three different predictive multicomponent mass transfer models for gas phase transfer, as follows:

MODEL I: based on an exact matrix method of solution to the Maxwell–Stefan diffusion equations for steady-state transfer across a "film",
MODEL II: based on the linearised theory of multicomponent mass transfer due to Toor and Stewart and Prober, and
MODEL III: in which it is assumed that each of the species acetone and benzene transfers independently of the other in the gas phase through a stagnant gas (nitrogen or helium).

For measured inlet conditions at the top of the wetted-wall column, the outlet conditions (temperature, compositions, net rates of transfer of acetone and benzene) predicted by the three different models above are compared with the experimentally determined values. It is seen that the predictions of Models I and II, both of which account for diffusional interactions in the vapour phase, show an average deviation of about 16% in the transfer rates. Model III, which utilizes a binary-type non-interacting mass transfer formulation, shows an average deviation of 50% for acetone and 39% for benzene transfers respectively. Furthermore, in one particular run (Run 7), this Model III completely fails to anticipate the correct direction of transfer of acetone; in this run reverse diffusion is experienced by acetone. The differences in the predictions of Models I and II are not found to be significant.

It is concluded that, for the system examined, diffusional interactions are present to a significant extent (this effect being more important for runs with helium as inert gas than for runs with nitrogen as carrier gas) and the ternary transfer behaviour is well predicted by multicomponent mass transfer models utilizing matrices of mass transfer coefficients including off-diagonal elements.

INTRODUCTION

Mass transfer phenomena are central to many problems in chemical engineering. Though many practical systems are multicomponent (here we define a multicomponent system as one in which the number of components exceeds two), most textbook treatments of mass transfer are largely restricted to two-component, or binary, systems[1]. There are important differences between binary and multicomponent mass transfer behaviour and before we consider the details of models for multicomponent mass transfer it is useful to recall some of these fundamental differences.

Let us first consider gas–liquid interphase mass transfer in a binary system made up of components 1 and 2. If N_1 and N_2 represent the molar fluxes of components 1 and 2, with respect to the gas–liquid interface, then it is usual to *define* the binary mass transfer coefficient for transfer in the gas phase by the relation (see Bird, Stewart and Lightfoot[2], page 658)

$$N_1 - y_{1b}(N_1+N_2) \equiv J_{1y} = k_y^{\bullet} \Delta y_1 \qquad (1)$$

for component 1. In equation (1) J_{1y} represents the bulk molar diffusion flux of component 1, with respect to the molar average reference velocity of the mixture; y_{1b} represents the bulk gas mole fraction; $k_y^{\bullet}$ is the binary mass transfer coefficient (the superscript black dot is used to emphasise the fact that this coefficient is dependent of the transfer fluxes N_i); Δy_1 is the driving force for mass transfer, taken here to be the difference between the bulk gas phase mole fraction and the interface composition, $\Delta y_i = y_{ib} - y_{il}$ (see Figure 1). We do not use the subscript y on the fluxes N_i because these fluxes are phase invariant.

If we consider the Stefan diffusion case, *i.e.* diffusion of component 1 through stagnant 2 (*i.e.* $N_2 = 0$) then it is easy to see that if we express the flux N_1 as

$$N_1 = \beta J_{1y} \qquad (2)$$

then β is a factor which is given by (*cf.* equation 1)

$$\beta \equiv 1/(1-y_{1b}) \qquad (3)$$

In general, whichever hydrodynamic model we choose (*e.g.* film, penetration, boundary layer, *etc*) to describe the mass transfer process, the (finite-flux) mass transfer coefficient $k_y^{\bullet}$ can be related to a zero-flux mass transfer coefficient k_y (representing conditions of vanishingly small mass transfer fluxes) by an equation of the form[2]:

$$k_y^{\bullet} = k_y \Xi \qquad (4)$$

0046–9858/81/010035–09 $02.00/0

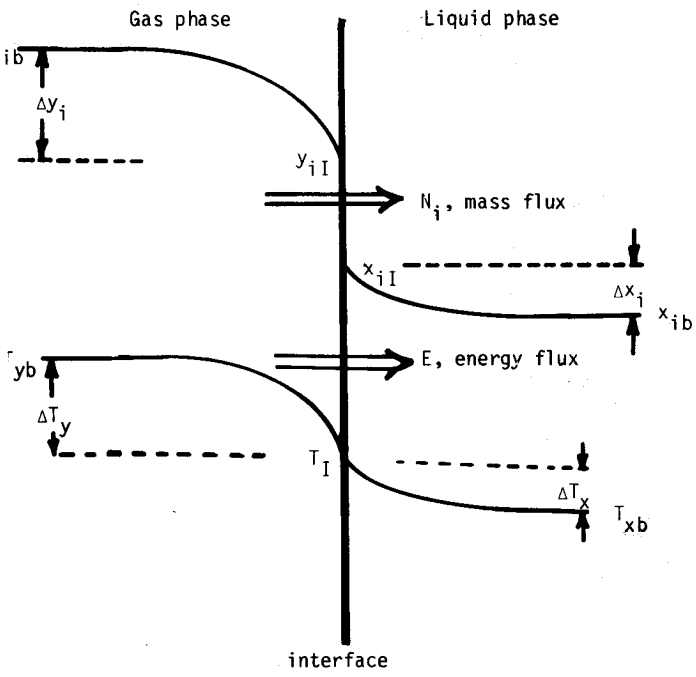

Figure 1. Composition and temperature profiles in the region of the gas–liquid interface.

where Ξ is a correction factor to account for the alteration to the composition profiles caused by finite transfer rates. If we adopt the film theory, for example, we obtain for the zero-flux transfer coefficient[2]

$$k_y = c_{ty}\mathscr{D}_y/\delta_y \tag{5}$$

and the finite flux correction factor Ξ is given as[2]

$$\Xi \equiv \Phi/(e^{\Phi}-1) \quad \text{where } \Phi \equiv N_t/k_y \tag{6}$$

Φ is the dimensionless mass transfer rate factor. It is easy to check that for vanishingly small mass transfer flux the mass transfer correction factor Ξ is unity and therefore the composition profiles in the film are linear.

The film thickness δ_y is usually unknown and therefore it is usual to estimate the zero-flux mass transfer coefficient k_y using a correlation of the form:

$$\frac{k_y}{(G_t/A_c)} = \frac{f}{2}(Sc_y)^{-2/3} \tag{7}$$

where Sc_y is the Schmidt number in the gas phase, $Sc_y = (\mu/\rho\mathscr{D})_y$; f, the Fanning friction factor, is a function of the Reynolds number; G_t (kmol/s) is the molar flow of the gases through a conduit of cross-sectional area A_c.

Let us now turn our attention to mass transfer between a ternary gas phase and a binary liquid phase, the gas phase consisting of components 1 and 2 which exchange mass with the liquid phase in the presence of an inert gas component 3. This is the multicomponent extension of the binary Stefan diffusion problem considered above. The description of the mass transfer process in the gas phase is complicated because of the fact that there are two independent driving forces Δy_1 and Δy_2; this is in contrast to the binary case above in which there is only one independent driving force ($\Delta y_2 = -\Delta y_1$ and $J_{2y} = -J_{1y}$ for a two-component system). The most general formulation of the interphase mass transfer relationship for the ternary mixture is the following:

$$N_1 - y_{1b}N_t \equiv J_{1y} = k^{\bullet}_{y11}\Delta y_1 + k^{\bullet}_{y12}\Delta y_2 \tag{8}$$

for component 1 transfer and analogously for component 2:

$$N_2 - y_{2b}N_t \equiv J_{2y} = k^{\bullet}_{y21}\Delta y_1 + k^{\bullet}_{y22}\Delta y_2 \tag{9}$$

where $k^{\bullet}_{yij}$ $(i,j = 1,2)$ are the multicomponent finite-flux mass transfer coefficients; Δy_i $(i = 1,2)$ are the driving forces for components 1 and 2, defined as the difference between the compositions in the bulk and the interface; N_t is the mixture total flux given by $N_t = N_1 + N_2$ (recall that $N_3 = 0$). Equations (8) and (9) can be written compactly in two-dimensional matrix notation as

$$(N) - (y_b)N_t \equiv (J_y) = [k_y^{\bullet}](\Delta y) \tag{10}$$

As in the binary case we can express the fluxes with respect to the interface, N_i, in terms of the diffusion fluxes J_{ij} as

$$(N) = [\beta_y](J_y) \tag{11}$$

where $[\beta_y]$, termed the bootstrap solution matrix[3], has its elements given by

$$\beta_{yij} = \delta_{ij} + y_{ib}/y_{3b}, \quad i,j = 1,2 \tag{12}$$

Exactly analogous to the binary case it is possible to write the finite flux mass transfer coefficients in terms of the zero-flux mass transfer coefficients and correction factors[3]

$$[k_y^{\bullet}] = [k_y][\Xi] \tag{13}$$

where $[\Xi]$ is the matrix of finite flux correction factors. Just as in the binary case both the zero flux coefficient $[k_y]$ and the correction factor matrix $[\Xi]$ depend on the model chosen to describe the mass transfer process[3]. Before proceeding to examine the models for predicting the mass transfer coefficients let us examine some consequences of the mass transfer relationships given by equations (8) and (9).

The coefficients $k^{\bullet}_{yij}$ $(i \neq j)$ are called cross-coefficients and these are in general non-zero and may have either positive or negative values. The main coefficients $k^{\bullet}_{yii}$ are usually positive. The presence of the cross-coefficients lends some bizarre characteristics to the multicomponent system[3]. Thus it may be possible to obtain reverse mass transfer ($J_{iy}/\Delta y_i < 0$), osmotic mass transfer ($J_{1y} \neq 0$ despite $\Delta y_1 = 0$), and mass transfer barrier ($J_{1y} = 0$ despite $\Delta y_1 \neq 0$). The phenomena of reverse mass transfer in which a component transfers in a direction opposite to that dictated by its own (intrinsic) driving force sets a multicomponent system apart from a simple two-component system. It is clear that the presence of the non-zero cross coefficients is responsible for the curious phenomena listed above, and may generally be termed as interaction phenomena. The interaction phenomena will be important for component 1, for example, when the term $k^{\bullet}_{y12}\Delta y_2$ is significant with respect to the term $k^{\bullet}_{y11}\Delta y_1$.

The above discussion serves to specify the objectives of the present paper. The first major objective is to determine whether interaction phenomena of the kind described

above can be significant for interphase mass transfer processes of interest to chemical engineers. In the present communication we analyse some experimental data measured by Modine[4] for mass transfer between a ternary gas phase consisting of acetone, benzene and nitrogen or helium and a binary liquid mixture of acetone and benzene in a wetted-wall column to obtain an indication of the interaction effects. The second objective of the present communication is to test the accuracy of some published multicomponent mass transfer models for the prediction of the coefficients $[k_y^\circ]$. The organization of the paper is as follows. We first examine some of the major models which have been suggested for the prediction of the multicomponent mass transfer coefficients. We then discuss the experimental set-up of Modine[4] and develop a procedure for the calculation of the mass transfer fluxes, using the various suggested mass transfer models. Finally the model predictions are compared with the experimental results of Modine[4]; these comparisons enable us to draw conclusions regarding the importance of diffusional interaction phenomena and of the accuracy of the various models. It must be remarked here that the model used by Modine to analyse his own ternary data is an outdated model by Toor[5]. Since this classic paper by Toor there have many new developments and models (see the review of Krishna and Standart[3]).

MODELS FOR MULTICOMPONENT MASS TRANSFER

We now examine three different models which have been suggested in the literature for the prediction of the multicomponent mass transfer coefficients.

MODEL I

The first model we consider is based on an exact matrix method of solution to the Maxwell–Stefan diffusion equations and is described in references 3 and 6 to 10. The matrix of zero-flux mass transfer coefficients is obtained as

$$[k_y] = [B_y]^{-1} \tag{14}$$

The elements of the matrix $[B_y]$ are given by

$$B_{y11} = y_{1b}/\mathscr{k}_{13} + y_{2b}/\mathscr{k}_{12} + y_{3b}/\mathscr{k}_{13} \tag{15}$$

$$B_{y12} = -y_{1b}(1/\mathscr{k}_{12} - 1/\mathscr{k}_{13}) \tag{16}$$

$$B_{y21} = -y_{2b}(1/\mathscr{k}_{12} - 1/\mathscr{k}_{23}) \tag{17}$$

$$B_{y22} = y_{2b}/\mathscr{k}_{23} + y_{1b}/\mathscr{k}_{12} + y_{3b}/\mathscr{k}_{23} \tag{18}$$

where $\mathscr{k}_{ij}$ ($ij = 12, 13, 23$) are the binary pair mass transfer coefficients, defined in the film model by

$$\mathscr{k}_{ij} \equiv c_{ty}\,\mathscr{D}_{yij}/\delta_y \tag{19}$$

$\mathscr{D}_{yij}$ is the binary gas phase diffusivity of the pair $i-j$ in the multicomponent mixture. It has been suggested by Krishna and Standart[6] that the correlation of the type given by equation (7) may be used to estimate the constituent binary pair mass transfer coefficient.

The matrix of finite-flux correction factors is given by

$$[\Xi] = [\Phi]\,[\exp[\Phi] - [I]]^{-1} \tag{20}$$

where the matrix of mass transfer rate factors $[\Phi]$ has elements given by

$$\Phi_{11} = N_1/\mathscr{k}_{13} + N_2/\mathscr{k}_{12} + N_3/\mathscr{k}_{13} \tag{21}$$

$$\Phi_{12} = -N_1(1/\mathscr{k}_{12} - 1/\mathscr{k}_{13}) \tag{22}$$

$$\Phi_{21} = -N_2(1/\mathscr{k}_{12} - 1/\mathscr{k}_{23}) \tag{23}$$

$$\Phi_{22} = N_2/\mathscr{k}_{23} + N_1/\mathscr{k}_{12} + N_3/\mathscr{k}_{23} \tag{24}$$

Notice the close similarities between the matrices $[B_y]$ and $[\Phi]$. For Stefan diffusion we have of course $N_3 = 0$ in equations (21) to (24).

The solution given by this model is exact for steady-state molecular diffusion across a film of thickness δ_y; for other cases this model is not exact.

MODEL II

This procedure for calculation of the mass transfer coefficients follows the linearised theory development of Toor[11] and Stewart and Prober[12]. In this procedure it is assumed that the matrix of multicomponent diffusion coefficients $[D_y]$, defined by the generalized Fick's law,

$$(J_y) = -c_{ty}[D_y]\,(\nabla y) \tag{25}$$

is constant along the diffusion path. For a multicomponent system the elements of $[D_y]$ are composition dependent, in contrast to the binary case, and have therefore to be evaluated at some average composition, usually the arithmetic average composition. We denote the arithmetic average matrix of diffusion coefficients as $[D_y]_{av}$; this has the elements (see [3]):

$$D_{y11} = \mathscr{D}_{13}(y_1\,\mathscr{D}_{23} + (1-y_1)\,\mathscr{D}_{12})/S \tag{25}$$

$$D_{y12} = y_1\,\mathscr{D}_{23}(\mathscr{D}_{13} - \mathscr{D}_{12})/S \tag{26}$$

$$D_{y21} = y_2\,\mathscr{D}_{13}(\mathscr{D}_{23} - \mathscr{D}_{12})/S \tag{27}$$

$$D_{y22} = \mathscr{D}_{23}(y_2\,\mathscr{D}_{13} + (1-y_2)\,\mathscr{D}_{12})/S \tag{28}$$

where the compositions y_i ($i = 1, 2, 3$) are to be taken as the arithmetic average between y_{ib} and y_{il}. S in equations (25) to (28) is given by

$$S = y_1\,\mathscr{D}_{23} + y_2\,\mathscr{D}_{13} + y_3\,\mathscr{D}_{12} \tag{29}$$

The matrix of zero flux mass transfer coefficients is then given by

$$[k] = c_{ty}[D_y]_{av}/\delta_y \tag{30}$$

or for forced convection mass transfer by a matrix relationship of the form

$$\frac{[k]}{(G_t/A_c)} = \frac{f}{2}\left[\frac{\rho_y}{\mu_y}[D_y]_{av}\right]^{2/3} \tag{31}$$

which is the matrix generalization of equation (7) and the matrix of zero-flux coefficients can be evaluated by the use of Sylvester's theorem[3]. It is important to appreciate the difference between Model II here and Model I. In Model I the pair binary mass transfer coefficients $\mathscr{k}_{ij}$ are evaluated from the correlation given by equation (7) whereas in Model II the matrix $[k]$ is evaluated directly from equation (31). Whereas Model I is exact within the limitations of the film model, Model II is an approxim-

ation even for this simple case (see Krishna and Standart[3] for a discussion on this point).

The matrix of correction factors is given for this case by

$$[\Xi] = [\Phi]_{av}[[\exp[\Phi]_{av} - [I]]]^{-1} \quad (32)$$

where $[\Phi]_{av}$ is defined as

$$[\Phi]_{av} \equiv N_t[k]^{-1} \quad (33)$$

It must be noted that when $N_t = 0$ (equimolar diffusion) the matrix $[\Phi]_{av}$ reduces to the null matrix and the matrix $[\Xi]$ reduces to the identity matrix. This is in contrast to the situation with Model I for which $[\Phi]$ does not reduce to the null matrix for $N_t = 0$; Model I therefore predicts finite flux corrections to the mass transfer fluxes even for equimolar diffusion.

MODEL III

In this model we adopt a pseudo-binary mass transfer formulation and assume that each component in the vapour phase transfers independent of the other in the presence of the inert gas. We therefore adopt mass transfer formulations of the form

$$J_{iy} = \not{k}_{i3}\,\Xi_i\,\Delta y_i, \quad i = 1,2 \quad (34)$$

where the correction factor Ξ_i is given as before by equation (6) with $\Phi_i = N_t/\not{k}_{i3}$. The zero flux mass transfer coefficient $\not{k}_{i3}$ is obtained from a correlation of the form given by equation (7) using the diffusivity $\mathscr{D}_{yi3}$ in the Schmidt number. It must be emphasised here that the commonly used Wilke effective diffusivity (see equation 18.4-25 of Bird *et al*[2]) for component i in a multicomponent mixture is only applicable for a transferring component in a mixture of stagnant species; see reference 3 for a discussion on this point. In the case under consideration both components 1 and 2 are transferring and the Wilke definition cannot be applied here. Also, in the experimental data to be analysed later, the components 1 and 2 are extremely dilute and therefore equation (34) may be expected to be a reasonable approximation.

TESTS OF THE MASS TRANSFER MODELS BY COMPARISON WITH EXPERIMENTAL DATA OF MODINE

Ternary mass transfer experimental data in vapour–liquid or liquid–liquid systems are very scarce. One comprehensive and accurate set of experimental data has been obtained by Modine[4]. Modine studied mass transfer between a binary liquid film of acetone and benzene flowing down a wetted-wall column and a co-currently flowing vapour stream containing acetone (1)–benzene (2) and nitrogen (3) or helium (3). Figure 2 gives a schematic diagram of the wetted-wall column used by Modine, whose thesis should be consulted for further details. The measured data are summarised in Table 1 (the original data of Modine have been converted to SI units before presentation in this table). The column was operated adiabatically. The column was 0.6096 m (24 inches) in length and the diameter was 0.025019 m (0.985 inch).

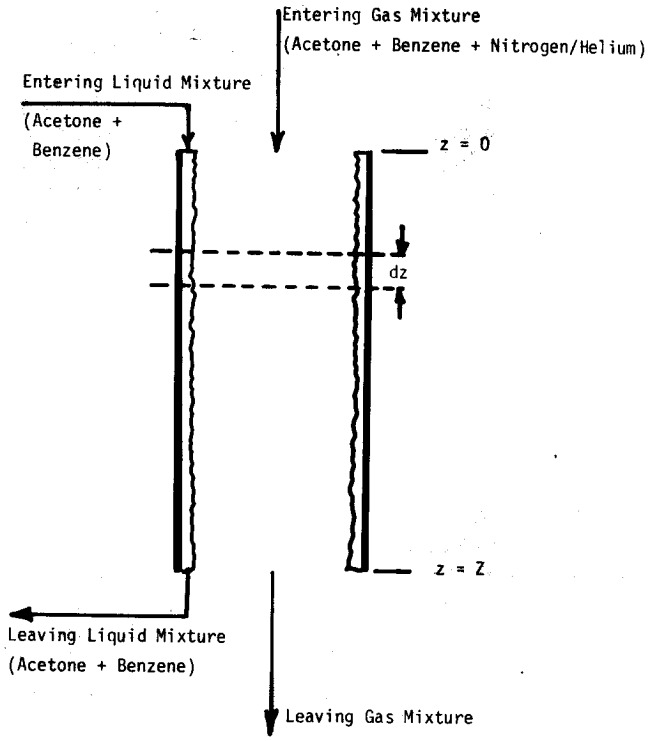

Figure 2. Schematic diagram of experimental set-up of Modine.

Modine, Parrish and Toor[13] have reported experimental correlations for binary mass transfer $\not{k}_y$ in the same column. The binary mass transfer data are of the form given by equation (7) with $f/2 = 0.0007 + 0.0625/(\mathrm{Re}_g)^{0.32}$; a correlation factor of 0.926 on the right-hand side of (7) fitted the experimental mass transfer data extremely well. This mass transfer correlation was used in this work to generate the mass transfer coefficients at any position in the wetted-wall column.

It is important to note that the conditions vary down the wetted-wall column as mass and heat transfer take place. The models described earlier give the mass transfer rates at any local position in the column. In order to obtain the composition and temperature profiles, it is necessary to set up and solve the proper material and energy balances in differential form along the height of the column.

MATERIAL BALANCES AND MASS TRANSFER RATES

The differential molar material balance for species i in the vapour phase takes the form

$$\frac{dG_i}{dz} = -N_i a A_c, \quad i = 1,2 \quad (35)$$

for acetone and benzene while for nitrogen or helium we have

$$\frac{dG_3}{dz} = -N_3 a A_c \quad (36)$$

In the liquid phase, which is a binary mixture of acetone and benzene, we have the material balance relationship

$$\frac{dL_i}{dz} = N_i a A_c, \quad i = 1,2 \quad (37)$$

Table 1. Wetted-wall column ternary experimental data of Modine (1963). Simultaneous heat and mass transfer between a downward flowing binary vapour + inert gas mixture and a falling binary liquid film

Run number	Inert gas	Liquid temp. (°C) Inlet	Liquid temp. (°C) Exit	Gas temp. (°C) Inlet	Gas temp. (°C) Exit	Column pressure (bar) Inlet	Column pressure (bar) Exit	Liquid flow L (gm s^{-1})	Carrier gas flow, G_3 (mol s^{-1})
1	Nitrogen	38.05	35.35	37.4	35.8	1.5499	1.4712	5.8223	0.0891404
2	Nitrogen	38.20	32.50	36.0	35.0	1.1943	1.0849	5.9219	0.0931459
3	Nitrogen	37.85	28.20	36.5	35.2	1.1956	1.0863	5.9723	0.1022607
4	Nitrogen	38.20	32.95	38.0	35.5	1.2529	1.1129	6.2810	0.1121410
5	Nitrogen	38.10	34.95	38.0	36.7	1.3176	1.1429	5.9219	0.1285733
6	Nitrogen	37.75	35.20	38.5	36.2	1.3842	1.1923	5.6573	0.1456165
7	Helium	36.45	21.00	36.0	33.5	1.2981	1.1368	5.5439	0.2438985
8	Helium	36.75	28.40	38.0	34.2	1.2888	1.1328	5.4317	0.2086600
9	Helium	37.70	33.50	37.8	35.6	1.1827	1.0827	5.8223	0.1067105
10	Helium	36.45	23.15	37.8	33.5	1.3187	1.1520	5.4872	0.2409764
11	Helium	36.20	19.05	38.0	34.1	1.2267	1.1227	5.7014	0.2917536

Run number	Inlet gas composition y_{1b}	Inlet gas composition y_{2b}	Exit gas composition y_{1b}	Exit gas composition y_{2b}	Inlet liquid x_{1b}	Exit liquid x_{1b}	Acetone condensed (mmol s^{-1})	Benzene condensed (mmol s^{-1})
1	0.123570	0.0	0.110154	0.029570	0.076529	0.099836	2.20947	−3.06404
2	0.145277	0.0	0.121959	0.037638	0.075939	0.100763	2.31470	−4.17159
3	0.081340	0.0	0.074216	0.032027	0.077432	0.081504	0.56274	−3.66440
4	0.137940	0.0	0.118906	0.031547	0.076537	0.104290	2.24729	−4.16417
5	0.180267	0.0	0.154831	0.030813	0.075998	0.121684	3.82927	−4.86487
6	0.176677	0.0	0.153830	0.026238	0.076581	0.128969	3.92832	−4.65973
7	0.052354	0.0	0.052120	0.018297	0.076583	0.079959	−0.20044	−4.77667
8	0.137716	0.0	0.122321	0.020769	0.078104	0.119976	2.73702	−5.06174
9	0.188229	0.0	0.167717	0.028604	0.091669	0.123758	2.33357	−3.79793
10	0.085668	0.0	0.079714	0.020633	0.090738	0.110859	1.34348	−5.52737
11	0.0	0.0	0.005406	0.016915	0.090610	0.074923	−1.61323	−5.04768

We use the convention in equations (35) to (37) that transfer from the vapour stream to the liquid stream (*i.e.* condensation) leads to a positive flux. A negative N_i would indicate evaporation.

In the liquid phase the transfer rates are simply given by

$$N_i = \ell_x^{\bullet}(x_{1i} - x_{1b}) + x_{1b}(N_1 + N_2) \tag{38}$$

The calculation of the rates of transfer N_i in the vapour phase can be carried out in various ways (Models I, II and III) as discussed earlier.

ENERGY BALANCE AND HEAT TRANSFER RATES

The variation of the bulk vapour temperature is described by the differential energy balance relationship

$$G_t C_p \frac{dT}{dz} = -q_y a A_c \tag{39}$$

where the conductive heat flux in the vapour phase is given by

$$q_y = h_y^{\bullet}(T_{yb} - T_i) \tag{40}$$

with the finite flux heat transfer coefficient in the vapour phase obtained by correcting the zero flux heat transfer coefficient for finite rates of mass transfer

$$h_y^{\bullet} = h_y \frac{\varepsilon}{\exp(\varepsilon) - 1} \tag{41}$$

where the dimensionless heat transfer rate factor ε, analogous to the dimensionless mass transfer rate factor Φ, is given by

$$\varepsilon = (N_1 C_{p1} + N_2 C_{p2})/h_y \tag{42}$$

The zero flux heat transfer coefficient can be obtained from a relation analogous to equation (7):

$$\frac{h_y A_c}{G_t C_{py}} = \frac{f}{2}(\mathrm{Pr})^{-2/3} \tag{43}$$

with $f/2$ given as the same function as the Reynolds number as for mass transfer.

The variation of the bulk liquid "film" temperature is given by

$$L_t C_{px} \frac{dT}{dz} = q_x a A_c \tag{44}$$

where the conductive heat flux in the liquid phase is given by

$$q_x = h_x^{\bullet}(T_i - T_{bx}) \tag{45}$$

The heat transfer coefficient in the liquid phase $h_x^{\bullet}$ was estimated by the method given by Modine, Parrish and Toor[13]. The interface temperature T_i is determined by an energy balance at the interface: $E_x = E_y$ or

$$q_x = q_y + (N_1(H_{1y} - H_{1x}) + N_2(H_{2y} - H_{2x})) \tag{46}$$

where H_i represents the partial molar enthalpy of the species i.

RESULTS AND DISCUSSIONS

A computer program using a finite difference approximation to the differential equations expressing the material and energy balances was used to calculate the compositions, temperatures, mass fluxes, *etc* along the length of the column. For this purpose the column length was divided into 24 equal segments (each of 1 inch) and the calculations performed assumed constant properties within each such segment.

The conditions corresponding to top of the column were taken to be the experimentally determined values. The physical and thermodynamic data used were the same as used by Modine and are given in detail elsewhere[14].

Table 2 gives a comparison of the experimentally determined conditions at the bottom of the column with the predictions of Models I, II and III. The net rates of transfer of acetone and benzene predicted by the three

Table 2. Comparison of experimentally determined outlet conditions with predictions of three different models

Run No.	Model	Gas temp. (°C)	Liquid temp. (°C)	Gas composition y_{1b}	Gas composition y_{2b}	Liquid composition x_{1b}	Acetone condensed (mmol s^{-1})	% deviation	Benzene condensed (mmol s^{-1})	% deviation
1	Experiment	35.80	35.35	0.11015	0.02957	0.09983	2.20947		−3.06404	
	Model I	36.84	34.74	0.11272	0.02820	0.10319	1.99551	−9.7	−3.02743	−1.2
	Model II	36.83	34.69	0.11271	0.02836	0.10319	2.00374	−9.3	−3.06119	−0.1
	Model III	36.84	34.70	0.10982	0.03107	0.10719	2.31848	+4.9	−3.35321	+9.4
2	Experiment	35.00	32.40	0.12196	0.03764	0.10076	2.31470		−4.17159	
	Model I	35.28	31.97	0.12573	0.03467	0.10288	1.95362	−15.6	−3.97421	−4.7
	Model II	35.25	31.86	0.12560	0.03509	0.10303	1.97110	−14.8	−4.04382	−3.1
	Model III	35.25	31.85	0.12199	0·03856	0·10835	2.38959	+3.2	−4.44329	+6.5
3	Experiment	35.20	28.20	0.07422	0.03203	0.08150	0.56274		−3.66440	
	Model I	34.63	28.61	0.07396	0.03218	0.08852	0.62083	+10.3	−3.79675	+3.6
	Model II	34.61	28.41	0.07386	0.03281	0·08869	0.62933	+12.0	−3.90259	+6.5
	Model III	34.61	28.40	0.07200	0.03469	0.09152	0.85038	+51.1	−4.11346	+12.2
4	Experiment	35.50	32.95	0.11890	0.03154	0.10429	2.24729		−4.16417	
	Model I	36.58	31.85	0.12047	0.03191	0.10374	2.07819	−7.5	−4.36567	+4.8
	Model II	36.58	31.74	0.12036	0.03232	0.10391	2.09649	−6.7	−4.44408	+6.7
	Model III	36.57	31.72	0.11721	0.03537	0.10913	2.53207	+12.7	−4.86203	+16.7
5	Experiment	36.70	34.95	0.15483	0.03081	0.12168	3.82927		−4.86487	
	Model I	37.20	33.95	0.15660	0.03024	0.12339	3.63045	−5.2	−4.95362	+1.8
	Model II	37.19	33.89	0.15660	0.03038	0.12338	3.64386	−4.8	−5.00077	+2.8
	Model III	37.19	33.84	0.15270	0.03417	0.13147	4.28690	+12.0	−5.62410	+15.6
6	Experiment	36.20	35.20	0.15383	0.02623	0.12896	3.92832		−4.65973	
	Model I	37.54	33.93	0.15418	0.02776	0.12997	3.92729	−0.0	−5.12142	+9.9
	Model II	37.54	33.87	0.15420	0.02785	0.12992	3.93808	+0.2	−5.16303	+10.8
	Model III	37.53	33.81	0.15069	0.03128	0.13849	4.58978	+16.8	−5.79703	+24.4
7	Experiment	33.50	21.00	0.05212	0.018297	0.07995	−0.20044		−4.77667	
	Model I	29.71	20.18	0.04979	0.023105	0.08872	+0.41047	−304.7	−6.24869	+30.8
	Model II	29.25	19.71	0.05017	0.023867	0.08740	+0.28531	−243.3	−6.48925	+35.8
	Model III	29.07	19.29	0.04668	0.02766	0.10133	+1.23571	−716.5	−7.52761	+57.6
8	Experiment	34.20	28.40	0.12232	0.02076	0.11997	2.73702		−5.06174	
	Model I	33.63	27.49	0.12130	0.02817	0.13462	3.69881	+35.1	−7.13207	+40.9
	Model II	33.59	27.54	0.12260	0.02708	0.12990	3,36796	+23.1	−6.89547	+36.2
	Model III	33.16	26.57	0.11242	0.03799	0.16700	5.94068	+117.0	−9.67810	+91.2
9	Experiment	35.60	33.50	0.16771	0.028604	0.12375	2.33357		−3.79793	
	Model I	35.24	31.91	0.16010	0.039960	0.13951	3.50785	+50.3	−5.50359	+44.9
	Model II	35.23	31.97	0.16242	0.03774	0.13534	3.19626	+36.9	−5.23177	+37.7
	Model III	34.81	31.08	0.14327	0.05794	0.16971	5.83519	+150.0	−8.04392	+111.8
10	Experiment	33.50	23.15	0.07971	0.02063	0.11085	1.34348		−5.52737	
	Model I	31.65	22.98	0.07862	0.02391	0.11930	1.53989	+14.6	−6.61407	+19.6
	Model II	31.43	22.83	0·07931	0.02387	0.11667	1.33224	−0.8	−6.63589	+20.1
	Model III	31.15	22.20	0.07355	0.03006	0.13991	2.92661	+117.8	−8.36271	+51.3
11	Experiment	34.10	19.05	0.00540	0.01691	0.07492	−1.61323		−5.04768	
	Model I	29.15	15.20	0.00575	0.01960	0.07520	−1.76538	+9.4	−6.01511	+19.1
	Model II	27.79	13.62	0.00627	0.02201	0.07381	−1.93535	+20.0	−6.79249	+34.6
	Model III	27.80	13.63	0.00631	0.02196	0.07360	−1.94954	+20.8	−6.77670	+34.2

Note 1. Model I: interfacial rates of transfer calculated using the Krishna–Standart multicomponent film model.
Model II: interfacial rates of transfer calculated using the Toor–Stewart–Prober multicomponent film model.
Model III: interfacial rates of transfer calculated using binary type, non-interacting, mass transfer model.

Note 2. % deviations calculated using

$$\% \text{ deviation} = \frac{(\text{predicted transfer rate} - \text{experimental transfer rate})}{(\text{experimental transfer rate})} \times 100$$

models are also compared with the experimentally measured values; the percentage deviations are given in Table 2. A good indication of the accuracy of Models I, II and III is obtained by comparing the average percentage deviations in the predictions of the rates of transfer, as given below.

	Model I (%)	Model II (%)	Model III (%)
Acetone transfer (excluding Run 7)	15.7	12.9	50.6
Benzene transfer	16.5	17.7	39.2

Models I and II are equally accurate and predict the rates of transfer to an accuracy of about 16%. Model III by comparison is extremely poor in its predictions showing deviations of between 39 to 51%. The first major conclusion to be drawn from this study is that diffusional interactions are extremely significant for the system studied. It can also be observed from Table 2 that the average deviations for the runs with helium as carrier gas are larger than for the runs using nitrogen as carrier. The reason for this is that the binary pair diffusivities in the vapour phase for the system acetone–benzene–helium differ to a greater extent than the corresponding values for the system acetone–benzene–nitrogen; the off-diagonal coefficients k_{12} and k_{21} are much larger for helium runs than for nitrogen runs. Model III of course ignores these off-diagonal elements altogether and it can be seen that this leads to large deviations for the helium runs using Model III. The experimental data must therefore be taken as confirming the importance of taking into account coupling or diffusional interaction effects. Put another way, the observed large differences between the deviations for the helium runs as compared to the nitrogen runs cannot be simply explained without allowing for off-diagonal elements in the mass transfer coefficient matrix $[k]$.

The experimental Run 7 with helium as carrier gas deserves special mention and attention. Here the predictions for the acetone transfer flux as predicted by all three models are poor. This large percentage deviation can be explained in part due to the extremely small magnitude of the absolute value of the acetone flux. We also see that all three models predict the wrong direction of transfer; while the experimental data show that there is net vaporisation of acetone, Models I, II and III predict net condensation of acetone. Let us examine the transfer behaviour in Run 7 more closely.

The variations of the vapour compositions and interfacial fluxes of acetone along the height of the wetted-wall column are shown in Figures 3 and 4. Figure 4 is very particularly interesting. It shows that while Models I and II predict that the interfacial acetone flux, N_1, changes sign in the column (from negative values at the top portion (vaporisation) to positive values towards the bottom of the column (condensation)), Model III anticipates that

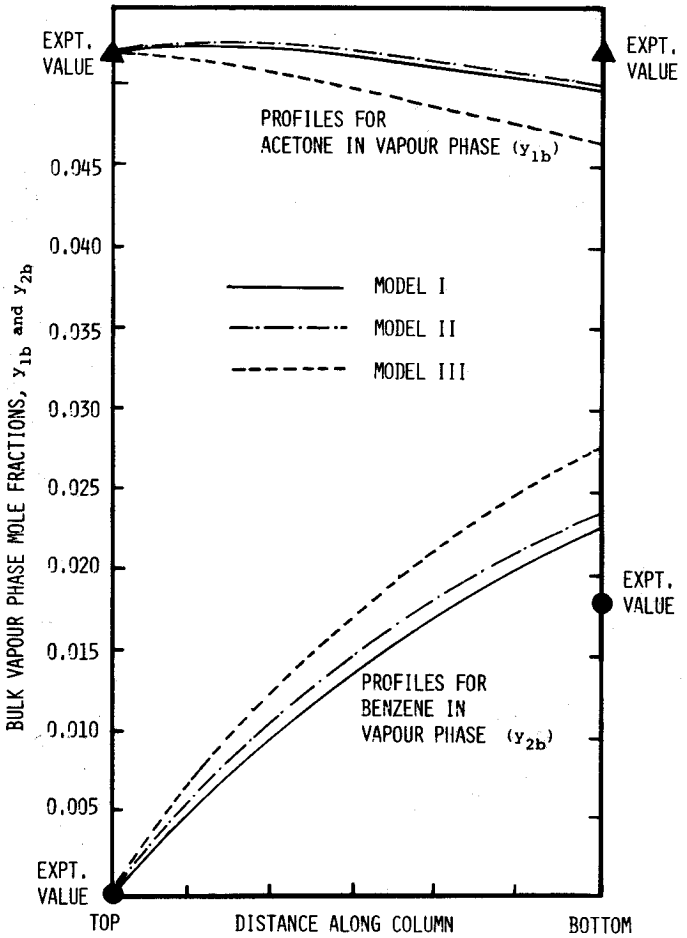

Figure 3. Acetone and benzene composition profiles along the length of the column for Run 7.

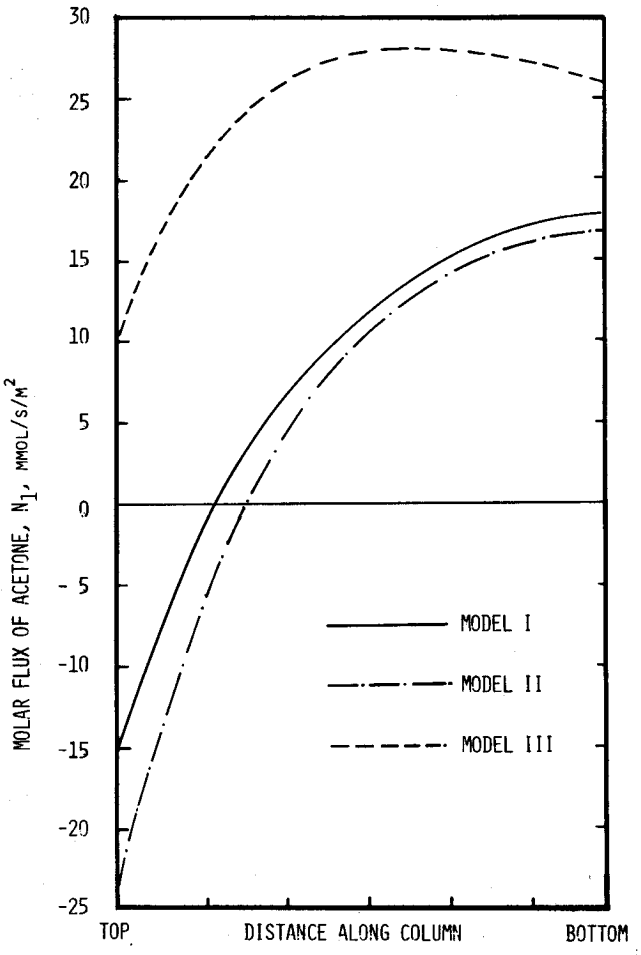

Figure 4. Acetone flux N_1 along the length of the column.

Table 3. Calculation of interfacial fluxes of mass and energy at the top of the wetted-wall column for Run 7. Comparison of values given by three different models

	Model I	Model II	Model III
Vapour phase compositions			
y_{1b}	0.052354	0.052354	0.052354
y_{1I}	0.037806	0.035718	0.041692
y_{1b}	0.000000	0.000000	0.000000
y_{2I}	0.131027	0.127744	0.125277
Vapour phase mass transfer coefficients $[k_y^*]$ (kmol m^{-1} s^{-1})			
k^*_{y11}	0.0021500	0.0017768	0.0022798
k^*_{y12}	0.0002648	0.0003155	0
k^*_{y21}	−0.0003322	0.0004531	0.
k^*_{y22}	0.0014474	0.0018527	0.0021533
Vapour phase diffusion fluxes, J_{iy} (kmol m^{-2} s^{-1})			
$J_{1y} \times 10^4$	−0.03412	−0.10741	0.24308
$J_{2y} \times 10^4$	−1.94488	−2.29132	−2.69765
Interfacial total molar fluxes, N_i (kmol m^{-2} s^{-1})			
$N_1 \times 10^4$	−0.14346	−0.23933	0.10747
$N_2 \times 10^4$	−1.94488	−2.29132	−2.69765
Temperatures, T(°C)			
T_{by}	36.00	36.00	36.00
T_i	33.25	32.60	32.48
T_{bx}	36.45	36.45	36.45
Interfacial energy flux, E (W m^{-2})			
E	6707.3	8069.7	8321.2

acetone will always condense everywhere in the column. This explains the large percentage deviation for the Model III prediction for net acetone transfer rate: −716%. Models I and II, on the other hand, predict successfully that vaporisation will occur in a portion of the column. The experimental data must therefore be taken as indicating the occurrence of reverse mass transfer in part of the length of the column. It is important here to stress that models assuming vanishing off-diagonal elements, *e.g.* Model III, cannot account for reverse mass transfer even qualitatively.

To explain the existence of reverse mass transfer in the column for Run 7 we consider the calculations by the three different models for the transfer at the top of the column where the gas and liquid phase are first brought into contact with each other. The calculations are summarised in Table 3. With Model I, the composition driving forces in the vapour phase are calculated as

$$\Delta y_1 = 0.014\underline{5}; \quad \Delta y_2 = -0.131\underline{0} \tag{47}$$

The driving force for mass transfer of component 2 (benzene) is about nine times as large as the driving force of component 1 (acetone) and of opposite sign. With the values of the finite flux mass transfer coefficients we see that the diffusion flux of acetone is given by

$$\begin{aligned} J_{1y} &= k_{11}^* \Delta y_1 + k_{12}^* \Delta y_2 \\ &= (0.002\underline{15})(0.014\underline{5}) + (0.000264\underline{8})(-0.131\underline{0}) \\ &= -0.000003412 \text{ kmol/s/m}^2 \end{aligned} \tag{48}$$

Thus while the driving force for acetone suggests that it should condense (transfer from the bulk gas phase to the interface), the calculations of the interacting model I suggests that the non-zero off-diagonal coefficient forces acetone to transfer against its intrinsic driving force, *i.e.* we have the situation that $J_{1y}/\Delta y_1 < 0$. Model II also predicts, rightly, the reverse mass transfer phenomenon for the point under consideration. The uncoupled mass transfer formulation Model III completely ignores the coupling effect and predicts a positive value for acetone, *i.e.* that there is net condensation of acetone. Experimentally it is observed that there is net vaporisation in the column and therefore reverse mass transfer must take place in some portion of the column, at least.

For Models I and II we have to subtract two large numbers to give a small net result (*cf.* equation 48) for the diffusion flux of acetone. The actual value of the diffusion flux J_{1y} predicted by the interacting mass transfer models will be especially sensitive to the value of the mass transfer coefficients k_{11} and k_{12}. This explains the large deviations for the net transfer rate of acetone in Run 7. The sensitivity in the determination of J_{1y}, and hence also N_1, is also reflected in the fact that Models I and II give the wrong overall direction of transfer. With a slightly different estimate of $[k]$, the correct direction of overall transfer could be predicted.

One aspect ignored in the above analysis presented above is the possible influence of Marangoni instabilities caused by surface tension gradients set up during mass transfer in the liquid phase. Such phenomena would tend to alter the liquid phase mass transfer coefficient and the interfacial area available for transfer. Considering the first effect, the alteration of the liquid phase transfer coefficient k_x would not significantly affect the results because the transfer process is predominantly gas film controlled. The alteration of the interfacial area would affect all the transfer rates in the same manner for all the three models. In our opinion, the conclusion reached here that the non-interacting model III is much inferior to the other two transfer Models I and II will not be altered. Finally, it must be said that because the changes in the liquid composition along the height of the column are very small (see Table 1), the surface tension gradients causing Marangoni instabilities, are also likely to be small.

CONCLUDING REMARKS

The experimental data obtained by Modine in a wetted-wall column for ternary mass transfer in the vapour–gas–liquid system comprising of acetone–benzene–nitrogen/helium indicate that diffusional interactions are present to a significant extent in this system. Such interactions are larger for the system with helium as inert gas than with nitrogen, this being explainable by a mass transfer model which includes off-diagonal elements. The predictive capabilities of multicomponent film Models I and II have been shown to be reasonably good, with average deviations in the region of 16%. Such models can be safely used in equipment design; the comparisons with experimental data show that the two multicomponent models are equally good in describing multicomponent mass transfer phenomena. The non-interacting Model III is hopelessly inadequate in describing the mass transfer process and such models are most probably too crude to use in equipment design, especially when the system is made up of components of widely differing molecular weights.

SYMBOLS USED

a interfacial area per unit volume of wetted-wall column, $a = 4/d_c (m^{-1})$
A_c cross-sectional area of wetted-wall column, $= \pi d_c^2/4 (m^2)$
$[B]$ matrix of inverted mass transfer coefficients ($kmol^{-1}\ m^2\ s$)
c_t total molar concentration of gas mixture ($kmol\ m^{-3}$)
C_p molar heat capacity of gas mixture ($J\ kmol^{-1}\ K^{-1}$)
d_c diameter of column ($=0.025019$ m $=0.985$ inch))
$[D]$ matrix of vapour phase diffusion coefficients ($m^2\ s^{-1}$)
$\mathscr{D}_{ij}$ diffusion coefficient in the vapour phase of binary pair i−j ($m^2\ s^{-1}$)
E energy flux, $= q + (N_1 H_1 + N_2 H_2)$ ($W\ m^{-2}$)
f Fanning friction factor
G_i molar flow rate of species i in the vapour phase ($kmol\ s^{-1}$)
G_t molar flow rate of vapour (+gas) mixture ($kmol\ s^{-1}$)
h heat transfer coefficient ($W\ m^{-2}\ K^{-1}$)
H_i partial molar enthalpy of species i in mixture ($J\ kmol^{-1}$)
$[I]$ identity matrix with elements δ_{ik}
J_i molar diffusion flux of species i relative to molar average reference velocity ($kmol\ m^{-2}\ s^{-1}$)
$[k]$ matrix of mass transfer coefficients ($kmol\ m^{-2}\ s^{-1}$)
k_{ij} mass transfer coefficient of binary pair i−j ($kmol\ m^{-2}\ s^{-1}$)
L_i molar flow rate of species i in liquid mixture ($kmol\ s^{-1}$)
L_t molar flow rate of total liquid mixture ($kmol\ s^{-1}$)
N_i molar flux of component i relative to a stationary coordinate reference frame ($kmol\ m^{-2}\ s^{-1}$)
N_t mixture molar flux relative to a stationary coordinate reference frame ($kmol\ m^{-2}\ s^{-1}$)
n number of species in mixture
Pr Prandtl number
q conductive heat flux ($W\ m^{-2}$)
R gas constant ($8314.4\ J\ kmol^{-1}\ K^{-1}$)
Re_g gas phase Reynolds number, $Re_g = d_c u_g \rho_g / \mu_g$
S summation constant defined by equation (29)
Sc_{ij} Schmidt number for binary pair i−j
T absolute temperature (K)
u_g superficial gas velocity ($m\ s^{-1}$)
x_i mole fraction of species i in liquid mixture
y_i mole fraction of species i in vapour mixture
Δy_i $= y_{ib} - y_{il}$, driving forces for mass transfer
(∇y) composition gradient vector, $n-1$ dimensional
z position coordinate along wetted-wall column, measured from top

Greek letters

$[\beta]$ bootstrap coefficient matrix
δ film thickness (m)
δ_{ik} Kronecker delta
ε heat transfer rate factor
μ viscosity of fluid mixture ($N\ s\ m^{-2}$)
Ξ_i pseudo-binary correction factor for species i
$[\Xi]$ matrix of correction factors
ρ mass density of fluid mixture ($kg\ m^{-3}$)
Φ dimensionless mass transfer rate factor for binary system
Φ_i pseudo-binary dimensionless mass transfer rate factor
$[\Phi]$ matrix of dimensionless mass transfer rate factors

Matrix notation

( ) $n-1$ dimensional column matrix
[ ] $n-1 \times n-1$ dimensional square matrix
$[\ ]^{-1}$ $n-1 \times n-1$ dimensional inverted matrix

Subscripts

av property evaluated at averaged conditions in diffusion layer
b bulk phase property
I interfacial property
t pertaining to total mixture
x pertaining to liquid phase
y pertaining to vapour phase

Superscript

* finite-flux coefficient

REFERENCES

1. Sherwood, T. K., Pigford, R. L. and Wilke, C. R., 1975, *Mass Transfer* (McGraw-Hill, New York).
2. Bird, R. B., Stewart, W. E. and Lightfoot, E. N., 1960, *Transport Phenomena* (Wiley, New York).
3. Krishna, R. and Standart, G. L., 1979, *Chem Engng Commun*, 3: 201.
4. Modine, A. D., 1963, *Ternary Mass Transfer*, PhD Dissertation, Department of Chemical Engineering, Carnegie Institute of Technology, Pittsburgh.
5. Toor, H. L. 1957, *AIChE J*, 3: 198.
6. Krishna, R. and Standart, G. L., 1976, *AIChE J*, 22: 383.
7. Krishna, R. and Panchal, C. B., 1977, *Chem Engng Sci*, 32: 741.
8. Krishna, R., Panchal, C. B., Webb, D. R. and Coward, I., 1976, *Letts Heat Mass Transfer*, 3: 163.
9. Krishna, R., 1977, *Chem Engng Sci*, 32: 659.
10. Krishna, R., 1979, *Letts Heat Mass Transfer*, 6: 137.
11. Toor, H. L., 1964, *AIChE J*, 10: 460.
12. Stewart, W. E. and Prober, R., 1964, *Ind Eng Chem Fundam*, 3: 224.
13. Modine, A. D., Parrish, E. B. and Toor, H. L., 1963, *AIChE J*, 9: 348.
14. Krishna, R., 1975, *Interphase Transport of Mass and Energy in Multicomponent Systems*, PhD Thesis, Dep of Chem Eng, University of Manchester Institute of Science and Technology.

ACKNOWLEDGEMENT

The author is grateful to Dr C. B. Panchal whose help with the computations has been invaluable and to Drs. Taylor and Webb, who in a private communication, derived the compact presentation of Equation (32).

ADDRESS

Correspondence concerning this paper should be addressed to: Dr R. Krishna at his present address: Koninklijke/Shell-Laboratorium, Amsterdam, Badhuisweg 3, 1031 CM Amsterdam, The Netherlands.

The manuscript of this paper was received 9 May 1980 and accepted for publication 19 September 1980 after small adaptations.